Journal of Biomechanics ∎ (∎∎∎∎) ∎∎∎–∎∎∎

Contents lists available at ScienceDirect

Journal of Biomechanics

journal homepage: www.elsevier.com/locate/jbiomech
www.JBiomech.com

In silico CDM model sheds light on force transmission in cell from focal adhesions to nucleus

Jean-Louis Milan [a,b,*], Ian Manifacier [a,b], Kevin M. Beussman [c], Sangyoon J. Han [c], Nathan J. Sniadecki [c], Imad About [a,b], Patrick Chabrand [a,b]

[a] Aix Marseille Univ, CNRS, ISM, Inst Movement Sci, Marseille, France
[b] APHM, Sainte-Marguerite Hospital, Institute for Locomotion, Department of Orthopaedics and Traumatology, Marseille, France
[c] University of Washington, Seattle, WA, USA

ARTICLE INFO

Article history:
Accepted 24 May 2016

Keywords:
Cytoskeleton
Nucleus deformation
Substrate stiffness
Microposts
Computational modeling
Divided medium mechanics
Mechanobiology
Mechanotransduction

ABSTRACT

Cell adhesion is crucial for many types of cell, conditioning differentiation, proliferation, and protein synthesis. As a mechanical process, cell adhesion involves forces exerted by the cytoskeleton and transmitted by focal adhesions to extracellular matrix. These forces constitute signals that infer specific biological responses. Therefore, analyzing mechanotransduction during cell adhesion could lead to a better understanding of the mechanobiology of adherent cells. For instance this may explain how, the shape of adherent stem cells influences their differentiation or how the stiffness of the extracellular matrix affects adhesion strength. To assess the mechanical signals involved in cell adhesion, we computed intracellular forces using the Cytoskeleton Divided Medium model in endothelial cells adherent on micropost arrays of different stiffnesses. For each cell, focal adhesion location and forces measured by micropost deflection were used as an input for the model. The cytoskeleton and the nucleoskeleton were computed as systems of multiple tensile and compressive interactions. At the end of computation, the systems respected mechanical equilibrium while exerting the exact same traction force intensities on focal adhesions as the observed cell. The results indicate that not only the level of adhesion forces, but also the shape of the cell has an influence on intracellular tension and on nucleus strain. The combination of experimental micropost technology with the present CDM model constitutes a tool able to estimate the intracellular forces.

1. Introduction

Controlling cell adhesion is a main aim in tissue engineering and biomaterials research. Indeed cell adhesion is a mechanobiological process which plays an epigenetic role influencing cell phenotype. During adhesion, transmembrane complexes such as integrins are able to connect specific proteins of the extra cellular matrix. This leads to creation and maturation of focal adhesions (FAs). Then cytoskeleton rearranges, forming stress fibers connecting FAs, and spatially organizes internal cellular organelles, such as the nucleus. FAs are able to withstand the actin-myosin contraction the cell produces to increase its stiffness and stability (Balaban et al., 2001; Del Rio et al., 2009). They are also the location for the initial mechanotransduction processes, via activation of talin, Rho-A kinase, involved in cytoskeleton contraction (Geiger et al., 2009; Wang et al., 2009). Cytoskeleton tension has been shown to play an important role in determining cell fate (McBeath et al., 2004; Bhadriraju et al., 2007; Kilian et al., 2010). Tension transmitted to the nucleoskeleton leads to nuclear deformation (Dahl et al., 2008; Nathan et al., 2011), opening of membrane ion channels and calcium entry and thereby inducing transcription of specific genes (Itano et al., 2003). Moreover, deformation of the nucleus causes repositioning of chromosomes and so affects gene transcription, as observed in cells whose nucleus is confined by both cytoskeleton and substrate microgrooved topography (McNamara et al., 2012). Understanding mechanotransduction during cell adhesion thus requires taking into account cytoskeleton tension, which appears to be a signal for mechanosensitive complexes from FAs to the nucleus.

Previous experimental works measured traction forces applied on focal adhesions (Tan et al., 2003; Fu et al., 2010; Legant et al., 2010; Rape et al., 2011). Novel techniques such as genetically encoded tension sensor microscopy or intracellular tomography were developed and give an insight in intracellular forces (Cost et al., 2015; Gayrard and Borghi, 2016; Hu et al., 2003). For

* Corresponding author at: APHM, Institute for Locomotion, GIBOC, Sainte-Marguerite Hospital, 270 Bd Sainte Marguerite 13274 Marseille, France. Tel.: +33 4 91 74 52 45; fax: +33 4 91 41 16 91.
E-mail address: jean-louis.milan@univ-amu.fr (J.-L. Milan).

http://dx.doi.org/10.1016/j.jbiomech.2016.05.031

instance, FRET-based tension sensor microscopy allows intracellular tension mapping at the molecular scale identifying regions of high and low tension. However, to date, this technology cannot quantitatively indicate the amount of force transiting through a given section of the cell. For this very reason we believe that the Cytoskeleton Divided Medium (CDM) model we proposed here can be a complementary tool to quantify forces transiting through the whole structure. Based on divided medium mechanics, the CDM model is an equilibrated system of multiple tensile and compressive interactions representing the "tensegrity like" nature of the cytoskeleton. It takes into account cell pre-stress and provides a discrete representation of the filaments of the cytoskeleton in opposition to continuum approaches of finite element modeling (Stamenović et al., 1996; Ingber 1997, 2003; Wendling et al., 2003; McGarry and Prendergast 2004; Maurin et al., 2008). Compared to classical tensegrity models, the CDM model possesses an evolving connectivity able to simulate cytoskeleton rearrangement by filament (dis)assembling (Milan et al., 2007). Stress fibers, actin cortex, microtubules, intermediate filaments and nucleoskeleton were also included in the model with specific mechanical role. The CDM model was used previously to analyze the influence of adherent shape on the mechanical state of the cell (Milan et al., 2013). This led to discriminant results yet still incomplete, because FA tractions were not measured. Indeed, a more precise computation of the intracellular mechanical state would depend on full knowledge of adhesion conditions, which must include the coordinates and forces applied on FAs. This is precisely the reason why we here combined FA traction measurement by micropost technology with a new optimization feature of the CDM model. This new feature enables the model to generate a traction force on each FA equal to what had previously been measured experimentally. With this approach, our scientific objective was to analyze the influence of substrate stiffness on the mechanical state of the cell. We considered 2 different stiffnesses of micropost arrays (Han et al., 2012). The computed cytoskeleton provided the internal distribution of intracellular tension and indicated the amount of force transmitted to the nucleus. As a result we obtain a non-trivial relationship between FA forces, intracellular tension, cell diameter and nucleus strain.

2. Materials and methods

The present CDM model is an improvement of the previous version (Milan et al., 2013) which only took cell shape into account. The CDM model has undergone extensive modifications for the sake of the present study to be cell-dependent and to act mechanically as the cell does. The new version uses FA traction measurements to simulate identical pulling forces, which the previous version did not. In the CDM model, the network of stress fibers is fully adaptable in terms of distribution, stiffness and contractility and is computed for each cell taking into account the real traction forces the cell exerts on the substrate. This is thought to better estimate the mechanical state of adherent cells.

2.1. Description of the CDM model

The CDM model represented a 15 μm diameter round cell with a 6 μm-diameter nucleus. Cell volume was divided into 12,000 spherical particles of diameters ranging between [0.4; 0.8] μm. Particle centers act as nodes of the network of interactions network within the divided medium. Nodes were classified by species: nucleus core, nucleus lamina, perinuclears, cell core, cell membrane, FAs (Fig. 1). Interactions between node species were ruled as a relationship between reaction force and gap (Milan et al., 2013). Two interaction laws, Elastic Wire and Contact, were used. Elastic Wire law acted like a virtual pre-strained elastic wire between two nodes: tension was proportional to stretching and became null when the elastic wire slackened. Contact law ruled interactions between the rigid spherical envelopes surrounding the nodes by generating necessary compression forces to prevent envelop interpenetration. The various components of the cytoskeleton and nucleoskeleton, were each modeled by specific interaction laws derived from the basic Elastic Wire and Contact laws (Supplementary Data Tables A and B). Nuclear lamina was reproduced by high-tensile LAMIN interactions between nuclear lamina nodes. Actin filaments were represented in by low-tensile interactions, termed

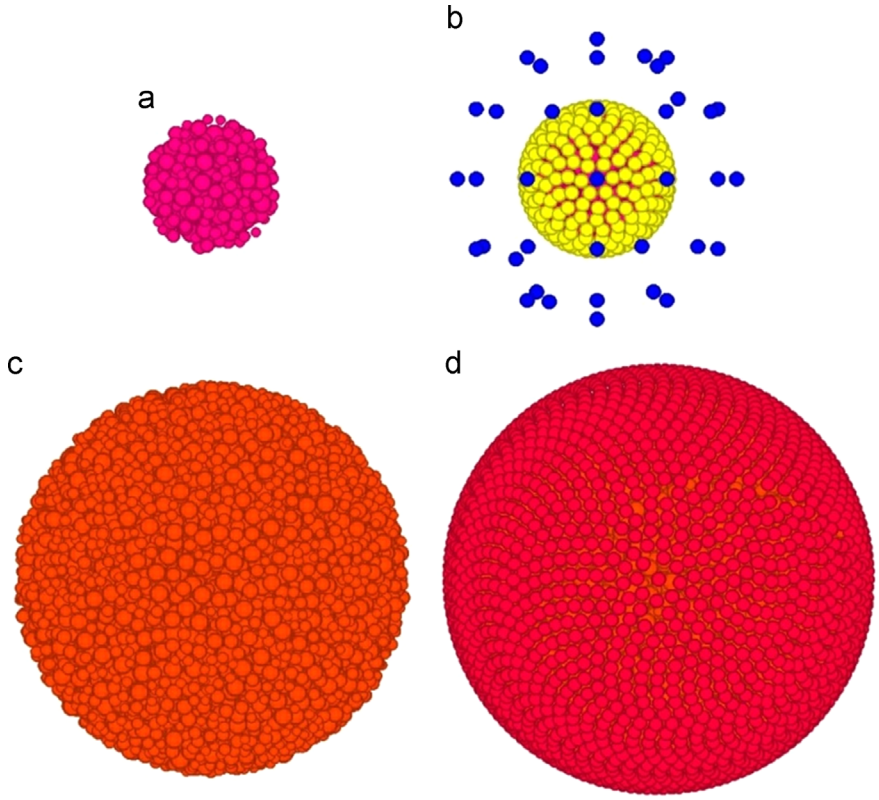

Fig. 1. Structure of the CDM model at round state (diameter=15 μm). Cell geometry is represented by a divided medium with nodes composed of different species: a) nucleus core (pink), b) nucleus membrane (yellow) and perinuclear nodes (blue) c) cell core nodes (orange) d) cell membrane (red). (For interpretation of the references to color in this figure legend, the reader is referred to the web version of this article.)

Please cite this article as: Milan, J.-L., et al., In silico CDM model sheds light on force transmission in cell from focal adhesions to nucleus. Journal of Biomechanics (2016), http://dx.doi.org/10.1016/j.jbiomech.2016.05.031

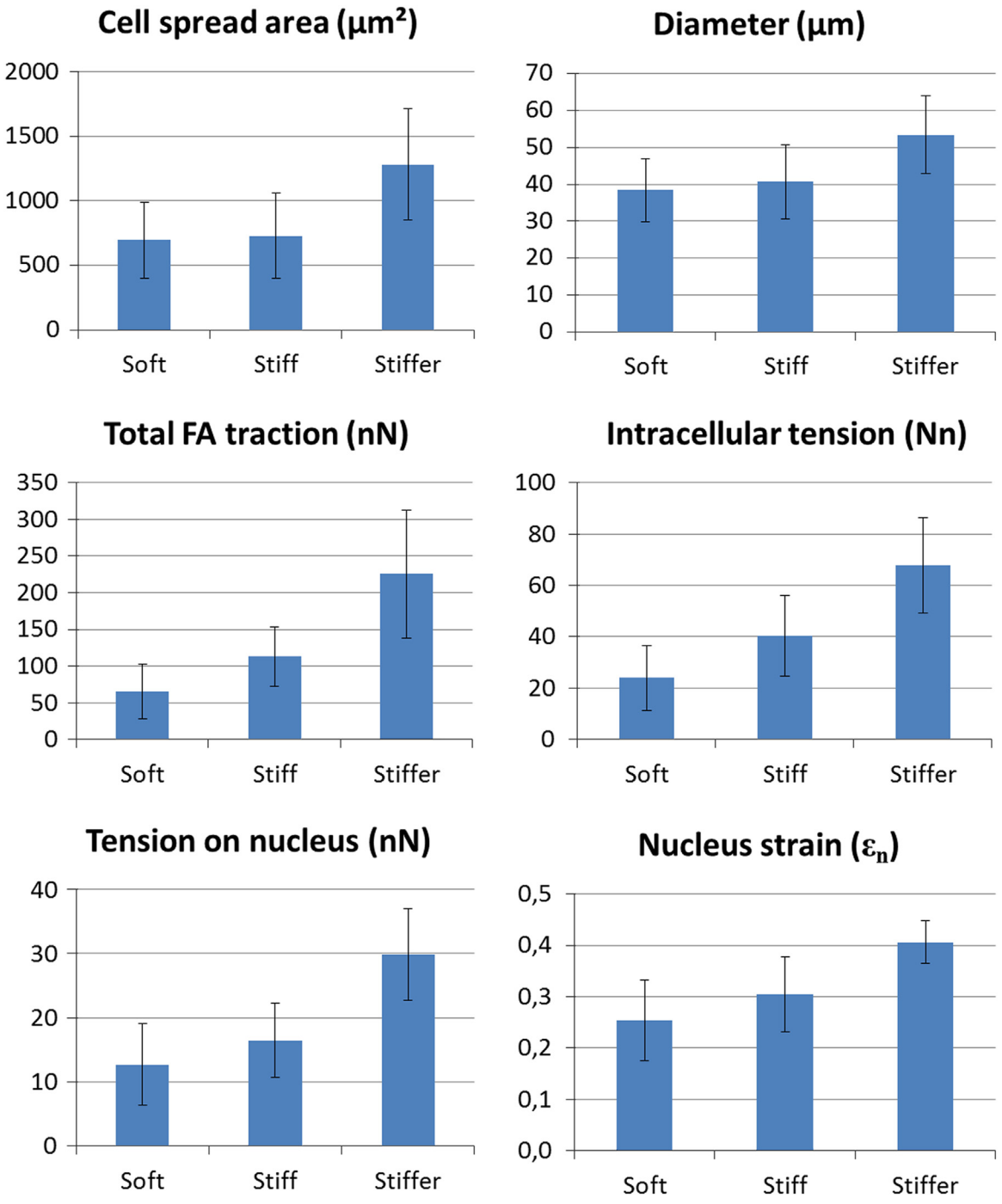

Fig. 2. Evolution of mean values of cell spread area, cell diameter, total traction, nucleus strain in cells cultured on the soft, stiff and stiffer substrates.

short F-ACTIN, creating cortical network between nodes of cell envelop as well as a diffuse network between cell core nodes. Actin filaments that form stress fibers were represented in the model by high-tensile interactions, termed long F-ACTIN, connecting focal adhesion nodes to perinuclear nodes and cortex nodes. A dense, yet initially slack network of INTER.FIL interactions surrounded the nucleus to represent intermediate filaments of the cytoskeleton. To match experimental descriptions (Green et al., 1986), INTER.FILs connected the long F-ACTINs to the nuclear LAMINs. Microtubules, which are also known to bear compression forces in cells (Brangwynne et al., 2006; Kurachi et al., 1995), were represented by MICROTUBULE law which was derived from Contact law and generated a compressive force network in the CDM model.

2.2. Cell cultures on soft and stiff micropost arrays

Computations of cytoskeleton structure and contractility were made for human pulmonary artery endothelial cells (HPAECs, Lonza) which were cultured on silicone microposts arrays for a previous study (Han et al., 2012). The deflection of a post was used to determine the local traction force of a cell (Lemmon et al., 2005). To analyze the influence of substrate stiffness on cells, soft and stiff micropost arrays were here considered. In the so-called soft substrate, microposts were 2.14 µm in diameter and 8.96 µm in height, leading to an average bending stiffness of 11 nN/µm. In the stiff substrate, microposts were 2.32 µm in diameter and 6.95 µm in height, leading to average bending stiffness of 31 nN/µm. Substrates were made of the same PDMS with a Young's modulus of 2.5 MPa measured according to ASTM standard D412. To extend the study, we analyzed the influence of a stiffer substrate. In the so-called stiffer substrate, microposts were 2.42 µm in diameter, 7.45 µm in height and made of PDMS with a Young's modulus of 3.2 MPa leading to a bending stiffness of 39 nN/µm. For the 3 substrates, the spacing between microposts was 9 µm center to center. Master arrays were made with SU-8 photoresist. Silicone arrays were manufactured via replica molding of polydimethylsiloxane (PDMS) using a mixing ratio of 10:1 for the base and curing agent (Sylgard 184, Dow Corning). The silicone arrays were stamped with 50 µg/ml fibronectin (BD Biosciences) to enable the attachment of cells. After seeding the

Please cite this article as: Milan, J.-L., et al., In silico CDM model sheds light on force transmission in cell from focal adhesions to nucleus. Journal of Biomechanics (2016), http://dx.doi.org/10.1016/j.jbiomech.2016.05.031

Table 1
Mean values of experimental measurements and computations of morphological and mechanical properties in the 25 cells using the CDM model. D and d, max and min cell diameters; $\Delta D/D0$, relative diameter variation of the model from initial spherical state to cell shape. D_n and d_n, max and min nucleus diameters.

Cells	Microposts	Soft	Stiff	Stiffer
In vitro cell measurements				
Spread area (μm²)		694	729	1282
Diameter (μm)		38	41	53
Aspect Ratio		1.02	1.10	1.12
FA number		16	18	25
Total FA traction (nN)		65	112	225
Mean traction on FA (nN)		4.4	6.5	10.2
Computational results				
Cell strain ($\Delta D/D_0$)		1.56	1.72	2.56
Cell strain (D/d)		1.12	1.10	1.19
Intracellular Tension T (Nn)		24	40	68
$T/T_{initial}$		6.8	11.5	19.4
T/Total FA traction		0.4	0.4	0.3
Computation results on nucleus mechanics				
Diameter (μm)		7.01	7.18	8.33
Strain	($\Delta dn/dn0$)	0.17	0.20	0.39
	Dn/dn	1.12	1.10	1.19
	ε_x	0.07	0.13	0.26
	ε_y	0.14	0.18	0.33
	ε_z	-0.43	-0.49	-0.57
	$\varepsilon_{nuclear\ shear}$	0.25	0.30	0.41
Tension on nucleus		12.73	16.49	29.88
Tension on nucleus/T		0.56	0.41	0.47

HPAECS onto the silicone arrays, they cells were cultured in F-12K Kaighn's modified media (Hyclone) containing 50 μg/ml ECGS (Biomedical Technologies, Inc), 100 μg/ml heparin (Sigma Aldrich), and 10% fetal bovine serum (Gibco). After culturing for 14 h on the arrays, the cells were permeabilized using Triton-extraction protocol and stained with Hoechst 33342 (Invitrogen), phalloidin (Invitrogen), IgG anti-vinculin (hVin1, Sigma Aldrich), and anti-IgG antibodies (Invitrogen). Images of the cells and microposts were obtained via fluorescence microscopy (Nikon TiE, 60 × oil objective, 1.4 NA). The spread area of a cell on an array was measured from an outline of its actin image. Locations of focal adhesions were determined from vinculin immunofluorescence while traction forces were calculated from micropost deflections.

2.3. Computation of cytoskeleton remodeling depending on real FA traction

As a compromise between statistical relevance and computation time, 10 cells were chosen for both the soft and stiff substrates conditions. 5 additional cells were chosen on the stiffer substrate to estimate the possible influence of additional stiffness. For each of the 25 cells, the CDM was forced to strain iteratively on the substrate until it connected the FA sites as described in (Milan et al., 2013); this is referred to as the spreading phase. Since adhesion forces are the signature of the contractile cytoskeleton we here sought to compute the cytoskeleton by taking into account experimentally measured FA forces. For the computed cytoskeleton to be valid, we considered that it should have same signature, i.e. that it should exert the same forces on the FA nodes as those measured using microposts. Finding the contractile properties for the modeled cytoskeleton can be seen as an inverse mechanics resolution which required an optimization process. We therefore considered that stress fibers connecting FA would be governed independently. At this stage, while long F-ACTIN interactions remained activated, we defined for each FA of number i (FA_i), a specific law of interaction SF_i between perinuclear nodes and FA_i (Supplementary Data Tables A & B). This means SF_i interactions connected intermediate filaments (INTER.FILs) surrounding the nucleus. Iteratively, SF_i stiffnesses were adjusted and the global equilibrium was computed using LMGC90 code (Dubois and Jean, 2006) until the cell model exerted the same FA traction forces as those measured experimentally. We started by defining all SF_i laws with a rigidity K_i set at 1 N/strain. For all following iterations, every K_i was multiplied by the ratio of the force magnitude computed at FA_i node over the experimental force magnitude. This local modification in SF_i rigidity not only changed the forces exerted on FA_i, but it affected the whole interaction network, and consequently the traction exerted on other FAs. For this reason, several iterations were required to reach convergence; computations were considered convergent when the relative differences between computed and experimental FA forces were less than 0.1% on average. This computational optimization is the remodeling phase of the cytoskeleton. Intracellular tension T, was computed as the sum of all Elastic Wire interaction forces through the plane located in the middle of the cell and perpendicular to the direction of maximum tension. To monitor in 3D the nucleus deformation, octahedral shear strain $\varepsilon_{nucleus\ shear}$ was computed as a norm of differences in nucleus strain in the 3 directions of space.

3. Results

Experimentally, from soft to stiff substrate, total FA traction increased, while cell spread area did not change significantly (Fig. 2 and Table 1). The stiffer substrate led to a strong increase of cell area and FA traction. Final computation results revealed an increase of intracellular tension in respect to the increase of substrate stiffness. Similar results were obtained for the amount of tension transmitted to the nucleus and for nucleus strain. Surprisingly the difference seemed even more important between the stiff and the stiffer substrate. The CDM model is shown in typical specimens of cells adhering on soft and stiff microposts in Figs. 3 and 4. During the spreading process, the mechanical state of the model changed and the number of active interactions increased. In the initial state, there were 50,000 non-null force interactions, while this number reached over 90,000 by the end of spreading. Over the whole cell sample, the spread configurations had more tensile interactions (short and long F-ACTIN and INTER.FIL) and less compressive interactions (MICROTUBULE). While SF interactions reached forces of about 30–70 pN in average with a maximum of 150 pN, the magnitude of other tensile and compressive interactions were only about 0.1–1 pN. From soft to stiffer substrate, stress fibers were more numerous and more contracted indicating a strengthening of the cytoskeleton with the substrate stiffness (Fig. 5). Stress fiber rigidities (K_i) are on average 50 and 70 times greater than their initial values, on soft and stiff substrate (Supplementary Data Table C).

The objective of iterative computation of cytoskeleton remodeling is to reduce the difference between the pulling force outputted by the model and the one measured experimentally for each FA. Over the whole sample of cells, only 10–20 iterations were required to converge and to generate a contractile cytoskeleton that delivered a mean FA force error of less than 0.1% (Fig. 6). On the other hand, there were very few FAs where the model was not able to yield results with such a high level of fidelity, which occasionally led to local errors lower than 10–30%, while in these cases additional iterations did not improve convergence.

With an initial value of 3.5 nN, the intracellular tension increased 7, 12 and 19 times in cells on soft, stiff, stiffer substrates at the end of cytoskeleton remodeling (Table 1). This increase in intracellular tension was partially transmitted to the nucleus via intermediate filaments (INTER.FILs). Initially slackened, INTER.FILs suddenly tightened under SF_i tension, becoming active bonds between the stress fibers and the nucleus. The tension transmitted to the nucleus reached respective averages of 13 nN, 17 nN and 30 nN on the soft, stiff and stiffer substrates (Table 1). This consequently led to further nucleus deformation. As expected, nucleus deformation ended up being higher on the stiff substrate compared to the soft one, results comparison between the stiff and the stiffest substrate further confirmed that stiffness has a positive effect on nucleus deformation (Fig. 2).

As expected, in the CDM model, intracellular tension correlated strongly (R^2=0.92) with total FA traction force (Fig. 7) being equivalent to 35% of total FA traction (Table 1). If nucleus strained linearly (R^2=0.86) with the tension transmitted to it, Fig. 7 shows that the tension transmitted to the nucleus correlated with intracellular tension (R^2=0.74). Nonetheless the shape of the cell also influences the local distribution of the intracellular tension and especially the tension transmitted to the nucleus. Indeed Fig. 7 also shows that nucleus deformation appeared to be equally dependent on cell diameter (R^2=0.723) and on intracellular tension (R^2=0.655). Since intracellular tension was related to the total FA

Please cite this article as: Milan, J.-L., et al., In silico CDM model sheds light on force transmission in cell from focal adhesions to nucleus. Journal of Biomechanics (2016), http://dx.doi.org/10.1016/j.jbiomech.2016.05.031

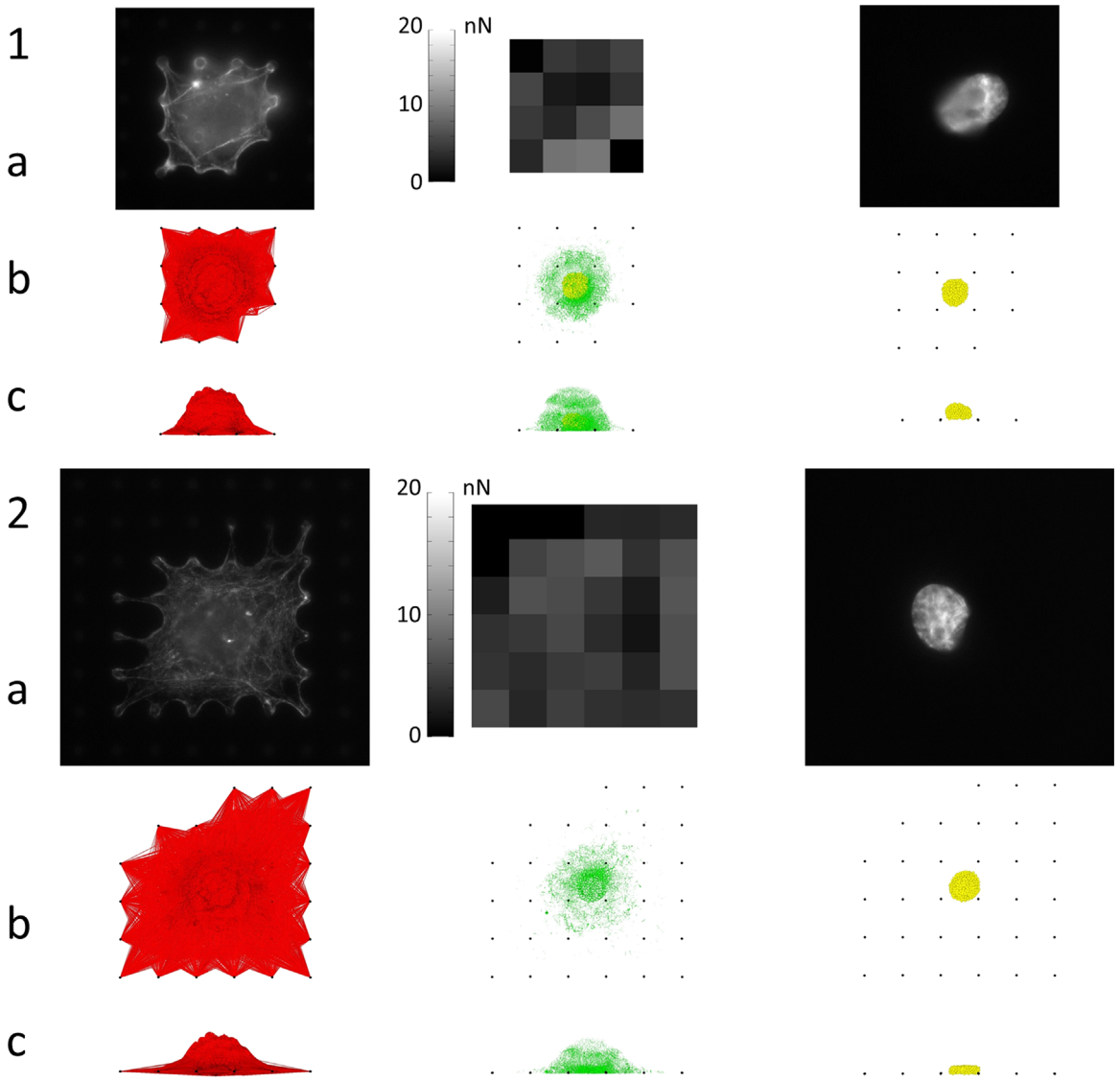

Fig. 3. Computational results in Cells 21 and 7 typical specimens of adherent cells cultured on (1) soft, (2) stiff micropost arrays respectively. a) Images of actin, nucleus and the spatial distribution of FAs and adhesion force magnitudes measured experimentally and used as input for the model. Spreading of the CDM model until it matched experimental adhesion conditions in top view (b) and side view (c); FA nodes in black, tensile interactions in red, compressive interaction in green; strained nucleus in yellow. Space between microposts is 9 μm. (For interpretation of the references to color in this figure legend, the reader is referred to the web version of this article.)

traction, we could define from computations, the following equation as an approximate relationship linking the nucleus strain to the cell diameter (D) and the total FA traction.

$$\varepsilon_{nucleusshear} = 0.0044\sqrt{TotalFAtraction.D} \quad (1)$$

Eq. (1) allows to estimate nucleus strain from experimental measurements of cell diameter and total FA traction. Over the whole cell sample, prediction of nucleus strain using (1) correlates positively (R^2=0.85) with nucleus strains computed by the model.

According to the model, these findings indicate that the cell shape has an influence on the distribution on intracellular forces, what may be more interesting is that the model indicates that the nucleus is not dissociated from this effect. Overall deformation of the nucleus may thus represent a mechanical signal during cell adhesion. Local deformation of the nucleus membrane, which was in average 9, 13, 15% in cells on soft, stiff and stiffer microposts respectively with a maximum of 100%, may also induce the cation channel opening involved in specific gene transcription. Since substrate stiffness modulates the net FA pulling force generated by adherent cells on substrate (Fig. 2), Eq. (1) may thus indicate the direct influence of substrate stiffness on nucleus strain.

4. Discussion

4.1. Representation of the contractile cytoskeleton in the CDM model

This multi-interaction model is a way to represent how the complex network of polymerized and reticulated cytoskeletal filaments interact to form an evolving mechanical structure of tensile and compressive forces. For instance, in cell 14 (stiffer substrate) the cytoskeleton was composed of 40,000 1 μm-actin filaments in a diffuse network, 12,000 10 μm-actin filament forming long stress fibers, 7,000 1 μm-microtubules forming long chains of compression while 1,200 elastic filaments composed the

Please cite this article as: Milan, J.-L., et al., In silico CDM model sheds light on force transmission in cell from focal adhesions to nucleus. Journal of Biomechanics (2016), http://dx.doi.org/10.1016/j.jbiomech.2016.05.031

nucleus lamina, all bearing individually forces generally between 1 and 10 pN.

The CDM model was not based on cytoskeleton imaging. On the contrary, Soiné et al. (2015) developed a 2D model which coupled traction force microscopy and stress fiber imaging to solve for intracellular tension. Similarly, our team developed a 2D model based on divided medium mechanics and actin imaging, to reconstruct the contractile structure of the whole actin network (Manifacier et al., 2016). Nonetheless, contrary to the CDM model, such models are currently not able to model interactions between actin filaments, microtubules and intermediate filaments, nor do they include measurement of tension forces on the nucleus.

In the CDM model, the distribution of stress fibers and their contractility are not initially imposed and result from optimization process. Fig. 8 displays the spatial arrangement of the stress fibers in the cell 14 adhering on the stiffer substrate. When it is compared to the actin image, the model shares similar principal orientation of stress fibers. Over the whole cell sample, model

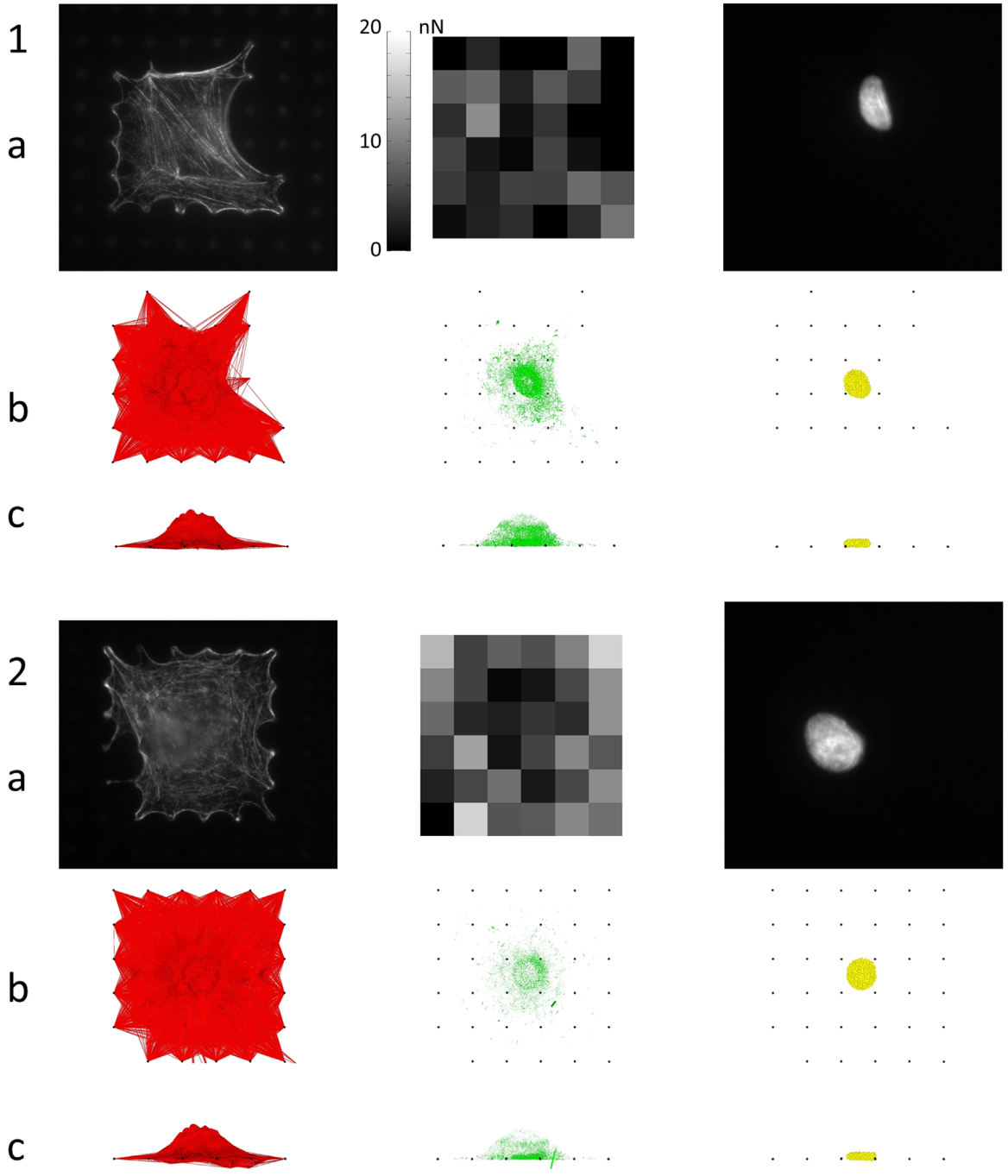

Fig. 4. Computational results in Cells 14 (1) and 15 (2) typical specimens of adherent cells cultured on the stiffer micropost array See Fig. 2 for description of a)–c). Space between microposts is 9 μm.

Please cite this article as: Milan, J.-L., et al., In silico CDM model sheds light on force transmission in cell from focal adhesions to nucleus. Journal of Biomechanics (2016), http://dx.doi.org/10.1016/j.jbiomech.2016.05.031

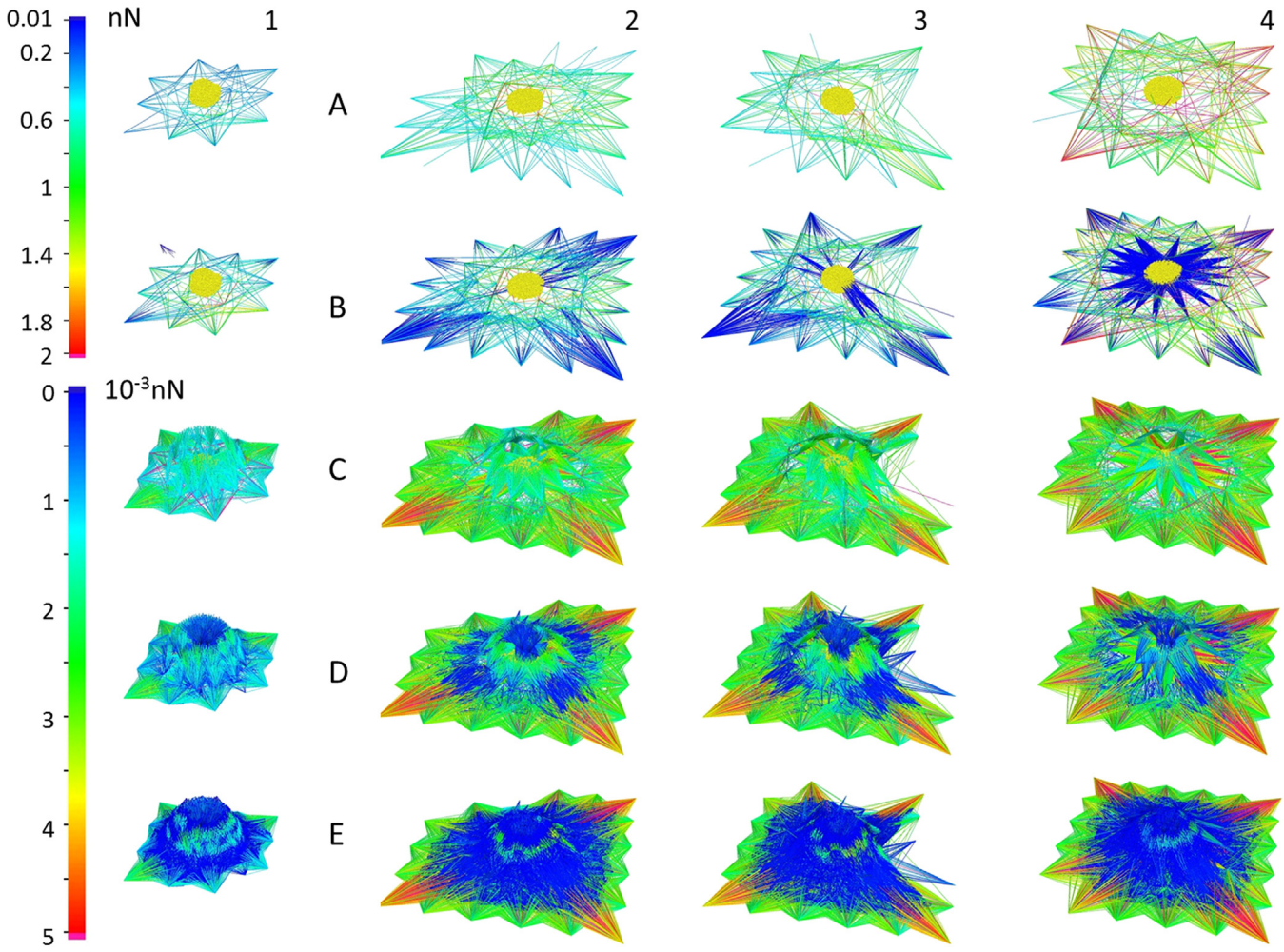

Fig. 5. Substructures of the contractile cytoskeleton computed by the CDM in the typical specimens of cells adhering on (1) soft, (2) stiff and (3,4) stiffer substrates. Substructures of the cytoskeleton depending on their level of tension: (A) 2-0.2 nN line; (B) 2 nN-5 pN; (C) 5 pN-0.1 pN; (D) 5 pN-0.01pN; (E) 5 pN-0.001 pN. Strained nucleus in yellow. (For interpretation of the references to color in this figure legend, the reader is referred to the web version of this article.)

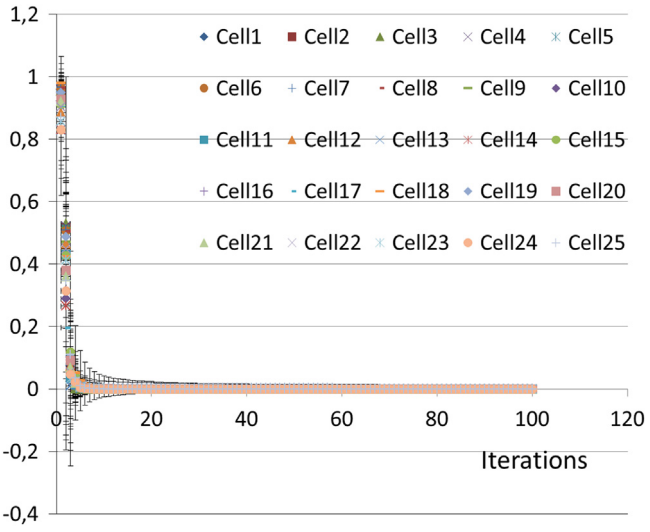

Fig. 6. Convergence of cytoskeleton remodeling computations in the whole sample of adherent cells. Evolution of mean relative error and standard deviation between computed and measured FA forces (ordinate) over iterations (abscise).

predictions of nucleus position differed by about only 5 μm in average from in vitro observations. The nuclear strain ratio (grand axis divided by the small axis) computed by the model only differed by about 25% in average.

4.2. Comparison between the present and previous version of CDM model

On Fig. 6, the first iteration corresponds to the model after spreading and before remodeling. This initial state corresponds to the previous configuration of the CDM model which was described and used in our precedent study (Milan et al., 2013). This initial state is associated with an important error in FA traction forces of about 80–100% in average compared to their experimental values. This means that the past CDM model cannot compute a cytoskeleton that behaves as the real one does. On the contrary, as depicted by Fig. 6, the iterative cytoskeleton remodeling process allows the CDM to closely mimic the pulling pattern of the observed cell. By incorporating in the model new conditions of cell-specific adhesion, we can safely assume that current results are more accurate than what we were able to present in our previous study.

Please cite this article as: Milan, J.-L., et al., In silico CDM model sheds light on force transmission in cell from focal adhesions to nucleus. Journal of Biomechanics (2016), http://dx.doi.org/10.1016/j.jbiomech.2016.05.031

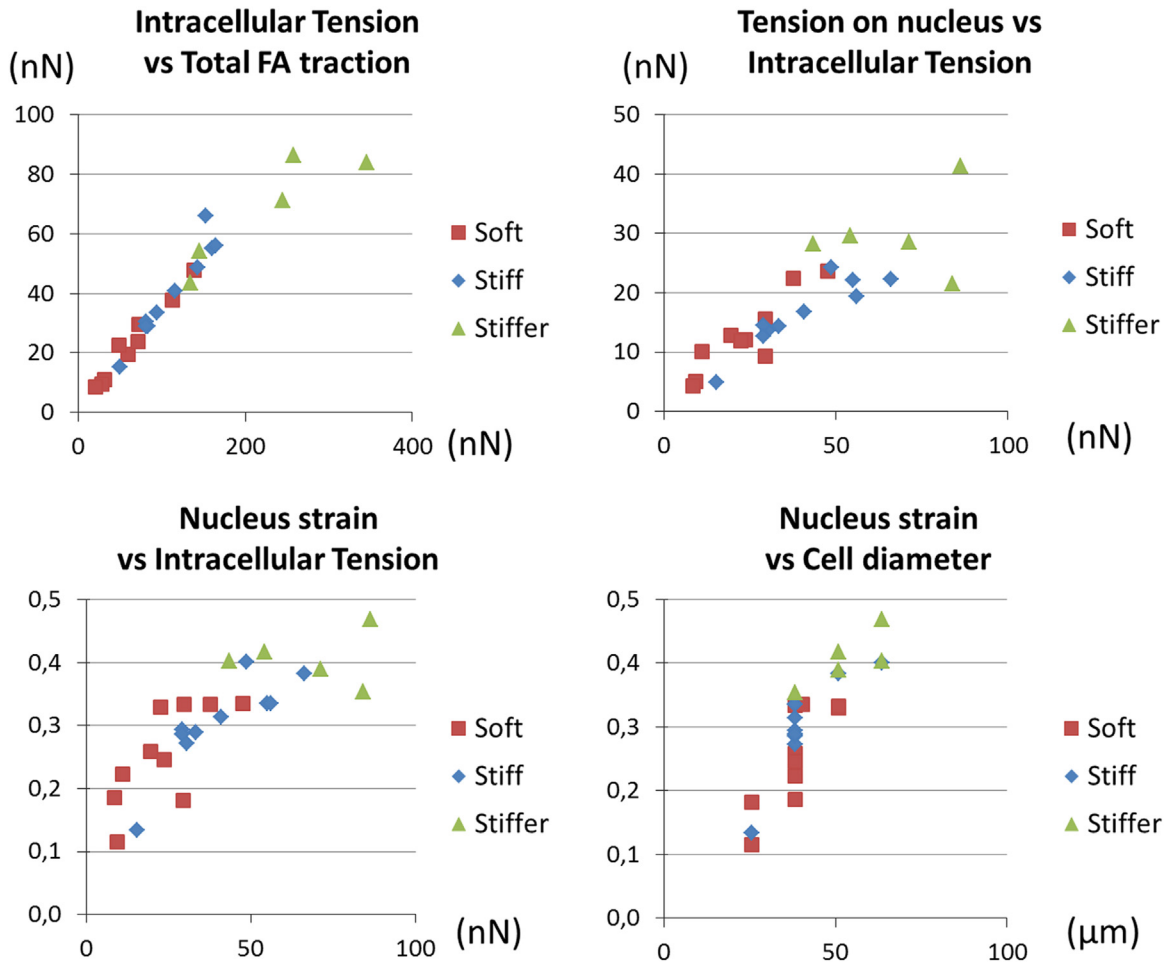

Fig. 7. Evolution of intracellular tension vs total FA traction on soft, stiff and stiffer substrates with a strong positive correlation (R^2=0.9201). Evolution of tension transmitted to nucleus vs intracellular tension on soft, stiff and stiffer substrates (R^2=0.7434). Evolution of nucleus strain vs intracellular tension (R^2=0.655) and vs cell diameter (R^2=0.723) on soft, stiff and stiffer substrates.

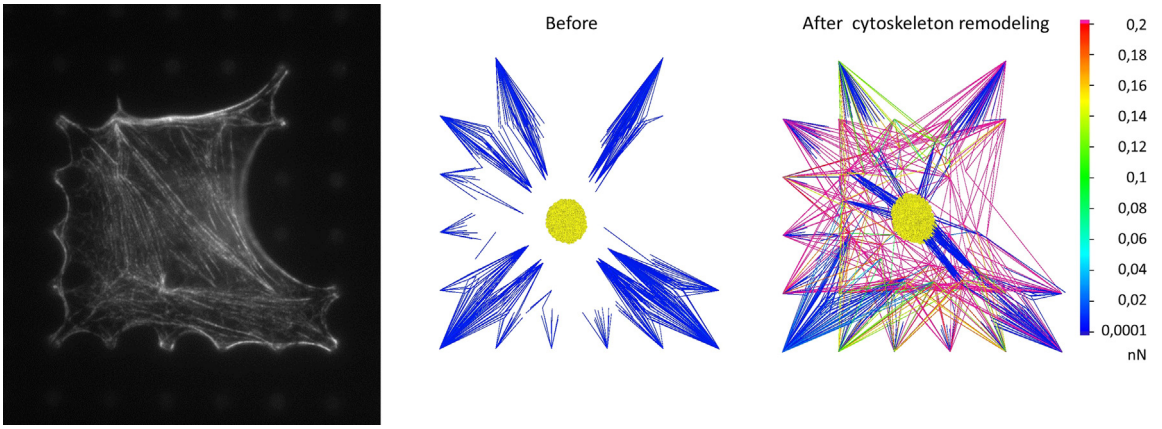

Fig. 8. In vitro vs in silico cytoskeleton. The real cytoskeleton of cell 14 which was cultured on stiffer substrate was imaged by immunofluorescence. The computed cytoskeleton is shown at the end of spreading phase, before and after cytoskeleton remodeling; only the sub-structures of the cytoskeleton corresponding to a range of force between 2 and 5 pN (B) are displayed.

4.3. CDM model and potential insight in cell mechanobiology

The CDM model is able to indicate how observable parameters such as nucleus strain, cell shape and FA forces interact, as experimentally observed (Han et al., 2012; McBeath et al., 2004). Additionally, CDM model is also able to take into account parameters that are currently unobservable, such as intracellular tension and the amount of force transmitted to the nucleus. For instance, the present study reveals the positive effect of cell spreading on the increase of tension transmitted to the nucleus.

Please cite this article as: Milan, J.-L., et al., In silico CDM model sheds light on force transmission in cell from focal adhesions to nucleus. Journal of Biomechanics (2016), http://dx.doi.org/10.1016/j.jbiomech.2016.05.031

Computed nuclear strain is equivalent to what has been experimentally observed as a possible factor modifying gene expression and inducing cell differentiation (Itano et al., 2003; Dahl et al., 2008; Nathan et al., 2011). By analyzing how nucleus shape and cytoskeleton tension interact, our study proposes potential parameters which could be involved in mechanotransduction during cell adhesion. For instance, the CDM model may indicate the influence of spreading compared to cytoskeleton remodeling on force transmission to the nucleus. At the end of spreading and before remodeling, nucleus strain ($\varepsilon_{nucleus\ shear}$) respectively averaged average 14%, 18% and 26% in cells cultured on soft, stiff, stiffer microposts. We found that after the remodeling phase, nucleus strained further up to 25% (soft), 30% (stiff) and 41% (stiffer). Similarly, after remodeling, the tensile load carried by intermediate filaments increased by a factor of 4–5 to reach, −12,7 nN (soft), −16,5 nN (stiff) and −29,9 nN (stiffer).

If Eq. (1) relates the nucleus strain only with FA traction forces and cell diameter, some additional computations launched on few star-shape cells from Yang et al. (2011) showed that nucleus strain may also depend on cell aspect ratio. The results are not shown because the size of the cell sample was not statistically significant.

5. Conclusion

The present study combines in vitro micropost technique and in silico CDM model to estimate the mechanical signals involved in cell adhesion. By considering microposts of different lengths, we show that substrate stiffness increases cell traction and that intracellular tension is neither directly, nor linearly transmitted to the nucleus. CDM model indicates the nucleus is more stimulated by tension forces in the case of highly spread cells, which in the case of stem cells is known to promote commitment into osteoblasts or fibroblasts. The present CDM model is able to compute the organization and contractility of cytoskeleton for every adherent cell and may contribute to further clarify mechanotransduction during cell adhesion.

Conflict of Interest Statement

The authors have declared that no competing interest exists in the present study

Acknowledgments

We acknowledge Michael Yang and Christopher Chen for providing additional experimental data of cell adhesion forces. The authors have declared that no competing interest exists.

Appendix A. Supplementary material

Supplementary data associated with this article can be found in the online version at http://dx.doi.org/10.1016/j.jbiomech.2016.05.031.

References

Balaban, N.Q., Schwarz, U.S., Riveline, D., Goichberg, P., Tzur, G., Sabanay, I., Mahalu, D., Safran, S., Bershadsky, A., Addadi, L., Geiger, B., 2001. Force and focal adhesion assembly: a close relationship studied using elastic micropatterned substrates. Nat. Cell Biol. 3, 466–472.

Bhadriraju, K., Yang, M., Alom Ruiz, S., Pirone, D., Tan, J., Chen, C.S., 2007. Activation of ROCK by RhoA is regulated by cell adhesion, shape, and cytoskeletal tension. Exp. Cell. Res. 313, 3616–3623.

Brangwynne, C.P., et al., 2006. Microtubules can bear enhanced compressive loads in living cells because of lateral reinforcement. J. Cell Biol. 173, 733–741.

Cost, A.L., Ringer, P., Chrostek-Grashoff, A., Grashoff, C., 2015. How to measure molecular forces in cells: a guide to evaluating genetically-encoded FRET-based tension sensors. Cell. Mol. Bioeng. 8 (1), 96–105.

Dahl, K.N., Ribeiro, A.J.S., Lammerding, J., 2008. Nuclear shape, mechanics, and mechanotransduction. Circ. Res. 102, 1307–1318.

Del Rio, A., Perez-Jimenez, R., Liu, R., Roca-Cusachs, P., Fernandez, J.M., Sheetz, M.P., 2009. Stretching single talin rod molecules activates vinculin binding. Science 323, 638–641.

Dubois, F., Jean, M., 2006. The non smooth contact dynamic method: recent LMGC90 software developments and application. Lecture Notes in Applied and Computational Mechanics, 27, pp. 375–378.

Fu, J., Wang, Y.K., Yang, M.T., Desai, R.A., Yu, X., Liu, Z., Chen, C.S., 2010. Mechanical regulation of cell function with geometrically modulated elastomeric substrates. Nat. Methods 7, 733–736.

Gayrard, C., Borghi, N., 2016. FRET-based molecular tension microscopy. Methods. 1 (94), 33–42.

Geiger, B., Spatz, J.P., Bershadsky, A.D., 2009. Environmental sensing through focal adhesions. Nat. Rev. Mol. Cell Biol. 10, 21–33.

Green, K.J., Talian, J.C., Goldman, R.D., 1986. Relationship between intermediate filaments and microfilaments in cultured fibroblasts: evidence for common foci during cell spreading. Cell. Motil. Cytoskelet. 6, 406–418.

Han, S.J., Ting, L.H., Bielawski, K.S., Rodriguez, M.L., Sniadecki, N.J., 2012. Decoupling substrate stiffness, spread area, and micropost density: a close spatial relationship between traction forces and focal adhesions. Biophys. J. 103 (4), 640–648.

Hu, S., Chen, J., Fabry, B., Numaguchi, Y., Gouldstone, A., Ingber, D.E., Fredberg, J.J., Butler, J.P., Wang, N., 2003. Intracellular stress tomography reveals stress focusing and structural anisotropy in cytoskeleton of living cells. Am. J Physiol. Cell Physiol. 285 (5), C1082–C1090.

Ingber, D.E., 1997. Tensegrity: the architectural basis of cellular mechanotransduction. Annu. Rev. Physiol. 59, 575–599.

Ingber, D.E., 2003. Tensegrity I. Cell structure and hierarchical systems biology. J. Cell Sci. 116, 1157–1173.

Itano, N., Okamoto, S., Zhang, D., Lipton, S.A., Ruoslahti, E., 2003. Cell spreading controls endoplasmic and nuclear calcium: a physical gene regulation pathway from the cell surface to the nucleus. Proc. Natl. Acad. Sci. USA 100, 5181–5186.

Kilian, K.A., Bugarija, B., Lahn, B.T., Mrksich, M., 2010. Geometric cues for directing the differentiation of mesenchymal stem cells. Proc. Natl. Acad. Sci. USA 107, 4872–4877.

Kurachi, M., Hoshi, M., Tashiro, H., 1995. Buckling of a single microtubule by optical trapping forces: direct measurement of microtubule rigidity. Cell. Motil. Cytoskelet. 30, 221–228.

Legant, W.R., Miller, J.S., Blakely, B.L., Cohen, D.M., Genin, G.M., Chen, C.S., 2010. Measurement of mechanical tractions exerted by cells in three-dimensional matrices. Nat. Methods 7, 969–971.

Lemmon, C.A., Sniadecki, N.J., Ruiz, S.A., Tan, J.T., Romer, L.H., Chen, C.S., 2005. Shear force at the cell-matrix interface: enhanced analysis for microfabricated post array detectors. Mech. Chem. Biosyst. 2 (1), 1–16.

Manifacier, I., Milan, J.L., Jeanneau, C., Chmilewsky, F., Chabrand, P., About, I., 2016. Computational tension mapping of adherent cells based on actin imaging. PLOS One. http://dx.doi.org/10.1371/journal.pone.0146863, Published: January 26.

Maurin, B., Cañadas, P., Baudriller, H., Montcourrier, P., Bettache, N., 2008. Mechanical model of cytoskeleton structuration during cell adhesion and spreading. J Biomech. 41, 2036–2041.

McBeath, R., Pirone, D.M., Nelson, C.M., Bhadriraju, K., Chen, C.S., 2004. Cell shape, cytoskeletal tension, and RhoA regulate stem cell lineage commitment. Dev. Cell 6, 483–495.

McGarry, J.G., Prendergast, P.J., 2004. A three-dimensional finite element model of an adherent eukaryotic cell. Eur. Cell Mater. 7, 27–33.

McNamara, L.E., Burchmore, R., Riehle, M.O., Herzyk, P., Biggs, M.J.P., Wilkinson, C.D. W., Curtis, A.S.G., Dalby, M.J., 2012. The role of microtopography in cellular mechanotransduction. Biomaterials 33, 2835–2847.

Milan, J.L., Wendling-Mansuy, S., Jean, M., Chabrand, P., 2007. Divided medium-based model for analyzing the dynamic reorganization of the cytoskeleton during cell deformation. Biomech. Model. Mechanobiol. 6, 373–390.

Milan, J.L., Lavenus, S., Pilet, P., Louarn, G., Wendling, S., Heymann, D., Layrolle, P., Chabrand, P., 2013. Computational model combined with in vitro experiments to analyze mechanotransduction during mesenchymal stem cell adhesion. Eur. Cells Mater. J. 25, 97–113.

Nathan, A.S., Baker, B.M., Nerurkar, N.L., Mauck, R.L., 2011. Mechano-topographic modulation of stem cell nuclear shape on nanofibrous scaffolds. Acta Biomater. 7, 57–66.

Rape, A.D., Guo, W.H., Wang, Y.L., 2011. The regulation of traction force in relation to cell shape and focal adhesions. Biomaterials 32, 2043–2051.

Soiné, J.R.D., Brand, C.A., Stricker, J., Oakes, P.W., Gardel, M.L., et al., 2015. Model-based traction force microscopy reveals differential tension in cellular actin bundles. PLoS Comput. Biol. 11 (3), e1004076.

Stamenović, D., Fredberg, J.J., Wang, N., Butler, J.P., Ingber, D.E., 1996. A microstructural approach to cytoskeletal mechanics based on tensegrity. J. Theor. Biol. 181, 125–136.

Tan, J.L., Tien, J., Pirone, D.M., Gray, D.S., Bhadriraju, K., Chen, C.S., 2003. Cells lying on a bed of microneedles: an approach to isolate mechanical force. Proc. Natl. Acad. Sci. USA 100, 1484–1489.

Wang, N., Tytell, J.D., Ingber, D.E., 2009. Mechanotransduction at a distance: mechanically coupling the extracellular matrix with the nucleus. Nat. Rev. Mol. Cell Biol. 10, 75–82.

Wendling, S., Cañadas, P., Chabrand, P., 2003. Toward a generalised tensegrity model describing the mechanical behaviour of the cytoskeleton structure. Comput. Methods Biomech. Biomed. Eng. 6, 45–52.

Yang, M.T., Reich, D.H., Chen, C.S., 2011. Measurement and analysis of traction force dynamics in response to vasoactive agonists. Integr. Biol. 3 (6), 663–674.

Please cite this article as: Milan, J.-L., et al., In silico CDM model sheds light on force transmission in cell from focal adhesions to nucleus. Journal of Biomechanics (2016), http://dx.doi.org/10.1016/j.jbiomech.2016.05.031